Soft Matter

RSC Publishing

PAPER

View Article Online
View Journal | View Issue

Immense elastic nonlinearities at the demixing transition of aqueous PNIPAM solutions

Cite this: *Soft Matter*, 2013, **9**, 5034

Martine Philipp,*[a] Ulrich Müller,[b] Ralitsa Aleksandrova,[b] Roland Sanctuary,[b] Peter Müller-Buschbaum[a] and Jan K. Krüger[b]

Elastic nonlinearities are particularly relevant for soft materials because of their inherently small linear elasticity. Nonlinear elastic properties may even take over the leading role for the transformation at mechanical instabilities accompanying many phase transitions in soft matter. Because of inherent experimental difficulties, only little is known about third order (nonlinear) elastic constants within liquids, gels and polymers. Here we show that a key concept to access third order elasticity in soft materials is the determination of mode Grüneisen parameters. We report the first direct observation of third order elastic constants across mechanical instabilities accompanying the liquid–liquid demixing transition of semi-dilute aqueous poly(*N*-isopropylacrylamide) (PNIPAM) solutions. Immense elastic nonlinearities, leading to a strong strain-softening in the phase-separating PNIPAM solutions, are observed. Molecular mechanisms, which may be responsible for these immense elastic nonlinearities, are discussed. The importance of third order elastic constants in comparison to second order (linear) elastic constants in the demixing PNIPAM solutions evidences the need to focus more on the general role played by nonlinear elasticity at phase transitions within synthetic and biological liquids and gels.

Received 4th January 2013
Accepted 20th March 2013

DOI: 10.1039/c3sm00034f

www.rsc.org/softmatter

A Introduction

For soft condensed matter, knowledge about its continuum mechanics plays a decisive role in understanding the molecular cohesion and organization.[1–21] When soft matter is subjected to a sufficiently small static strain, the mechanical response is controlled by linear elastic, but not viscoelastic, properties.[21] If liquids, gels or polymers are excited by a dynamical mechanical probe, their viscoelastic properties become relevant. This relevance increases with the complexity of the molecular structure in terms of inter- and intramolecular degrees of freedom. At sufficiently high probe frequencies, often lying in the upper MHz or GHz regime, the mechanical relaxation processes are dynamically clamped and the mechanical response of the system is purely elastic again. Hence, for soft materials the mechanical response may be of linear elastic nature when probed either statically or at sufficiently high probe frequencies. In such case, it can be described by Hooke's law, using the second order elastic constants (SOECs) provided by the linear elastic stiffness tensor of 4^{th} order.

Of course linear elasticity only describes one aspect of the complex mechanical behaviour of soft matter. The regime of linear elastic response is often soon abandoned for soft materials as the stress or strain amplitude is increased in stress–strain or dynamic mechanical experiments (*e.g.* ref. 4–6, 8 and 11–14). In order to quantify this nonlinear elastic response of the material within the frame of continuum mechanics, Hooke's law must be extended. Usually the consideration of third order elastic constants (TOECs), but no higher order elastic constants, is sufficient to describe the nonlinear elastic response.[21,22]

Because of the usually small SOECs of liquids, gels and polymers, it is obvious that nonlinear elastic properties often play a more crucial role in soft matter than in hard condensed matter. The large number of investigations dealing with the nonlinear elastic properties of synthetic and biological soft materials proves that the importance of elastic nonlinearities for a better understanding of soft matter is generally accepted (*e.g.* ref. 1–21). Most of these investigations, based on stress–strain experiments or rheology, give essential insight into the specific nonlinear mechanical response of complex synthetic and biological soft materials. The corresponding experiments are rarely treated within the frame of elasticity theory of mechanical continua. Hence, the nonlinear elastic susceptibilities, *i.e.* third and higher order elastic constants, are seldom quantified during these investigations. Exceptions are reported for example in ref. 15, 18 and 19, where Brillouin spectroscopy, applied *e.g.* on strained polymers, yields the full third order elastic stiffness tensor.

Similar to hard condensed matter (*e.g.* ref. 23–25), knowledge about TOECs can be of immense value for the better

[a]*Technische Universität München, Physik-Department, Lehrstuhl für Funktionelle Materialien, James-Franck-Strasse 1, D-85748 Garching, Germany. E-mail: martine.philipp@tum.de; Fax: +49 89 289 12473; Tel: +49 89 289 12455*

[b]*Université du Luxembourg, Laboratoire de Physique des Matériaux, Campus Limpertsberg, L-1511 Luxembourg, Luxembourg*

understanding of molecular cohesion and organisation in soft matter. In particular, the testing of theoretical concepts, for instance related to the Landau theory of phase transitions,[22] may demand for quantitative values of TOECs. Experimental investigations of TOECs at transformation phenomena in soft matter are rare; examples exist for the thermal glass transition in polymers.[17,26,27] The so-called ferroelastic phase transitions,[22] for which the mechanical stress is the order parameter, are particularly fascinating from the mechanical viewpoint. For such transitions, a linear elastic constant is interpreted as the inverse order parameter susceptibility and therefore strongly softens at the phase transition. A mechanical instability hence accompanies such phase transitions. It is however unclear which role TOECs play for such ferroelastic phase transitions in soft matter.

Corresponding mechanical instabilities were reported for the ferroelastic demixing transition of poly(*N*-isopropylacrylamide) (PNIPAM) hydrogels and aqueous PNIPAM solutions.[3,20,28,29] At the demixing temperature T_c, the homogeneous low-temperature phase separates into PNIPAM-rich and PNIPAM-poor domains.[20,28–52] In the course of this phase separation, the longitudinal modulus c_{11} strongly decreases.[20,28,29] The PNIPAM solutions possess large mechanical instabilities, for which $\Delta c_{11}/c_{11}$ may already reach 17% for a 6 mass% PNIPAM solution.[20] It could be shown that for PNIPAM solutions at T_c, the relationship between the longitudinal modulus and mass density $c_{11}(\rho)$ is drastically altered.[20] In particular, the steep decrease of the $c_{11}(\rho)$-curve proves that the large variations of the longitudinal modulus at T_c are not at all governed by the evolution of the mass density. Thus, the important variation of the longitudinal modulus at T_c is not dominated by variations of the mass density, but of the intermolecular and intramolecular 'spring constants', *i.e.* the changing elastic interactions within the phase-separating solutions. Note that these strongly changing 'spring constants' as a function of density can qualitatively be interpreted in terms of the occurrence of elastic nonlinearities. Hence, concrete indications exist that significant elastic nonlinearities rise at the demixing transition of aqueous PNIPAM solutions.

The present article deals with the quantitative determination of TOECs across the liquid–liquid demixing transition of semi-dilute aqueous PNIPAM solutions. In order to overcome the inherent tremendous experimental difficulties of measuring TOECs within liquids, we apply a key concept, which is well-known from solid state physics: the mode Grüneisen parameter[16,17,21,26,27,53,54] (see Section C.2). Brillouin spectroscopy[55,56] is used as the main experimental method. We report the first direct observation of the evolution of TOECs at the mechanical instability accompanying a liquid–liquid phase transition. A significantly widened perspective on this mechanical instability allows for a deeper insight into the molecular mechanisms governing the demixing transition of PNIPAM solutions. The detected immense TOEC at the demixing transition of PNIPAM solutions evidences the need to focus in more detail on the role played by nonlinear elasticity at phase transitions within synthetic and biological soft matter.

B Experimental

B.1 Materials

Linear poly(*N*-isopropylacrylamide) (PNIPAM) homopolymer with a number average molecular weight of 20–25 kg mol^{-1} was purchased from Sigma-Aldrich Chemie GmbH, Taufkirchen, Germany. The polymer has a purity of 97%. The contour length of a single PNIPAM molecule corresponds to about 44 nm and in aqueous environment its radius of gyration amounts to a few nanometers.[30,34] Semi-dilute aqueous poly(*N*-isopropylacrylamide) (PNIPAM) solutions with a concentration of 3 and 6 mass% were prepared in cleaned glass vials using Millipore water. After shaking these solutions for some hours, they were stored in the fridge for several days in order to become completely transparent and homogeneous. The demixing transition of these solutions is of the lower critical solution temperature type.[20,28–45] The demixing temperature T_c lies for both solutions between 33 and 34 °C.[20,28–45]

B.2 Brillouin spectroscopy

Brillouin spectroscopy is a light scattering technique which is used here to investigate acoustic properties of liquids at gigahertz frequencies.[20,55–58] Hence, this technique measures dynamically clamped acoustic properties, so that viscoelasticity does not play a role. It is an invasive and non-destructive technique. In this application of Brillouin spectroscopy, the photons of laser light are inelastically scattered on thermally induced hypersonic waves, also called acoustic phonons, propagating within the sample. The term 'acoustic phonon' originally stems from lattice vibrations in crystals. However, this concept can also be transferred without any restriction to amorphous materials, if the employed acoustic wavelength largely exceeds interatomic distances. This holds true for the present study, as the involved acoustic wavelength amounts to about 200 nm.

The light, which is inelastically scattered from the sample, is analyzed using a tandem Fabry–Pérot interferometer as a high resolution tunable optical filter. Brillouin spectra are recorded for a fixed wave vector $\vec{q}$, defined by the employed scattering geometry. The magnitude of the wave vector amounts to 0.032 nm^{-1} in the current investigation. The position of the Brillouin doublet in the Brillouin spectrum yields the frequency and its line width the temporal attenuation of the involved hypersonic wave. Originally Brillouin spectroscopy was used to determine the hypersonic properties of transparent single crystals and liquids. Modern tandem Fabry–Pérot interferometers have such a high optical contrast (of 10^5 to 10^6) that they are even able to analyse the inelastically scattered light of translucent or opaque samples. This feature is essential for the present study, where the hypersonic properties of highly opaque, demixed PNIPAM solutions are characterized. If the heterogeneities leading to the optical opacity are small in comparison to the probing acoustic wavelength, information about the average hypersonic properties of the heterogeneous material is gained.

The kinematic description of the inelastic scattering of light photons by acoustic phonons is as follows. Applying the law of energy conservation to the inelastic scattering process, the hypersonic frequency f of the probed acoustic phonons can be

related to the angular frequencies, ω_s and ω_i, of the scattered and incident light, respectively, according to:

$$\hbar\omega_s = \hbar\omega_i \pm 2\pi\hbar f. \quad (1)$$

Similarly the law of momentum conservation relates the wave vector $\vec{q}$ of the probed acoustic phonon to the wave vectors $\overrightarrow{k_s}$ and $\overrightarrow{k_i}$ of the scattered and incident light according to:

$$\hbar\overrightarrow{k_s} = \hbar\overrightarrow{k_i} \pm \hbar\vec{q}. \quad (2)$$

The selected scattering geometry defines the wave vector $\vec{q}$. Hence the frequency f of the hypersonic wave is the response of the system for a chosen wave vector $\vec{q}$. In order to optimize the scattering intensity for the current studies, the backscattering geometry was selected. In this configuration, the magnitude of the wave vector q^{180} of the probed hypersonic wave, or its wavelength Λ^{180}, depends on the refractive index of the scattering volume n_{λ_0} according to:

$$q^{180}(T) = 2\pi/\Lambda^{180}(T) = 4\pi n_{\lambda_0}(T)/\lambda_0. \quad (3)$$

The vacuum wavelength of the used frequency-doubled Nd-YAG Verdi laser from Coherent, USA equals to $\lambda_0 = 532$ nm. Refractive indices *versus* temperature are given in ref. 20 for the PNIPAM solutions. As these values only slightly vary with temperature at the demixing transition, the magnitude of the wave vector is almost constant for each sample. This constancy of the wave vector is of great importance for the calculation of mode Grüneisen parameters, which are the basis for the determination of TOECs (see Section C.2).

The longitudinal hypersonic velocity $v_L(T)$ of the propagating sound waves is given by:

$$v_L(T) = f_L^{180}(T)\Lambda^{180}(T) \approx f_L^{180}(T)\cdot\lambda_0/2n_D(T). \quad (4)$$

In Voigt notation,[59] the longitudinal elastic modulus of an isotropic system is expressed by (for details, see Section C.1):

$$c_{11}(T) = \rho(T)v_L^2(T). \quad (5)$$

All measurements were carried out on a highly modified and software-controlled six-pass tandem Brillouin spectrometer from JRS Scientific Instruments, Switzerland. Details about the experimental setup and the Brillouin spectroscopic investigations are given in ref. 20.

B.3 Densitometry

The measurements of the mass density *versus* temperature were carried out with a DMA 5000 M densitometer from Anton Paar, Austria. According to the manufacturer, the statistical error of the mass density lies below 10^{-5} g cm^{-3} and absolute temperature accuracy better than 0.1 °C is achieved.

C Theoretical background

C.1 Continuum mechanics

The basic equation for elasticity is obtained by a Taylor expansion of the elastic free energy F_{el} (written in Voigt notation):[21]

$$F_{el}(T, V_0\varepsilon_1, \ldots, V_0\varepsilon_6) = F_0 + 1/2V_0\sum_{ij} c_{ij}\varepsilon_i\varepsilon_j + 1/6V_0\sum_{ijk} c_{ijk}\varepsilon_i\varepsilon_j\varepsilon_k + o(\varepsilon_i^4) \quad (6)$$

F_0 denotes the elastic part of the free energy in the unstrained elastic continuum, V_0 a reference volume, ε_i the components of the elastic strain tensor, c_{ij} the components of the second order elastic stiffness tensor, c_{ijk} the components of the third order elastic stiffness tensor and $o(\varepsilon_i^4)$ the neglected fourth and higher order terms. From the equations of state $\sigma_i(T,V_0\varepsilon_1, \ldots, V_0\varepsilon_6) = 1/V_0\partial F/\partial\varepsilon_j|_{T,\varepsilon_{j\neq i}}$, where σ_i denotes the six components of the stress tensor, the elastic susceptibilities c_{ij} and c_{ijk} can be derived:

$$c_{ij} = 1/V_0\partial^2 F/\partial\varepsilon_i\partial\varepsilon_j|_{T,\varepsilon_{k\neq i,j}} = \partial\sigma_i/\partial\varepsilon_j|_{T,\varepsilon_{k\neq j}}, \quad (7)$$

and

$$c_{ijk} = 1/V_0\partial^3 F/\partial\varepsilon_i\partial\varepsilon_j\partial\varepsilon_k|_{T,\varepsilon_{l\neq i,j,k}} = \partial^2\sigma_i/\partial\varepsilon_j\partial\varepsilon_k|_{T,\varepsilon_{l\neq j,k}}. \quad (8)$$

The susceptibilities c_{ij} are called second order elastic constants (SOECs) and appear in Hooke's law. The susceptibilities c_{ijk} are called third order elastic constants (TOECs) and reflect the nonlinear elastic contributions to the equations of state. As long as the nonlinear part in eqn (6) yields a negligible contribution to F_{el}, there is no need to consider the TOECs. Hooke's law is then sufficient to describe the elastic properties of the considered material. Note that it is the ratio between nonlinear and linear elasticity which decides about the relevance of nonlinear elasticity rather than the absolute values of the SOECs and TOECs.[21,22]

The number of independent SOECs and TOECs depends on the macroscopic symmetry of the sample. For isotropic materials two independent SOECs exist: the longitudinal modulus c_{11} and the shear modulus c_{44}.[21,59] For liquids, the shear modulus is zero. For the macroscopically isotropic state, the third order elastic tensor contains only six components: c_{111}, c_{112}, c_{123}, c_{144}, c_{155} and c_{456}. According to the isotropy conditions, only three of those TOECs are independent:[21] $c_{112} = c_{123} + 2c_{144}$, $c_{155} = c_{144} + 2c_{456}$ and $c_{111} = c_{123} + 6c_{144} + 8c_{456}$.

In conclusion, if Hooke's law strictly holds true for a given system, the elastic response functions, *i.e.* the SOECs c_{ij} or linear combinations of them, do not depend on the applied strain and hence all higher order elastic constants vanish. For a liquid, like an aqueous solution of PNIPAM, possessing a zero shear modulus, Hooke's law predicts that the only remaining SOEC $c_{11} > 0$ GPa should not depend on volume or density. This statement is the basis for the introduction of mode Grüneisen parameters (see Section C.2). If under the given experimental conditions the elastic response function depends on volume (or density), then elastic nonlinearities must be taken into account.

C.2 Mode Grüneisen parameter

Mode Grüneisen parameters were originally introduced in solid state physics to access lattice anharmonicities of single

crystals.[16,17,21,26,27,53,54] The definition of the mode Grüneisen parameter of an acoustic mode with polarization p and a wave vector $\vec{q}$ is as follows:

$$\gamma(p,\vec{q}) = \partial \ln f(p,\vec{q})/\partial \ln \rho = \rho/f(p,\vec{q})\partial f(p,\vec{q})/\partial\rho. \quad (9)$$

The mode Grüneisen parameter accesses in linear response the variation of the frequency f of a given acoustic mode while changes of the mass density ρ occur. In the case of mode Grüneisen parameters, the lattice anharmonicity, or elastic nonlinearity, is thus not measured by a classical stress–strain experiment, but *via* the change of the frequency of an acoustic mode induced by a variation of density. Indeed, the infinitesimal variation of the frequency f, provoked by an infinitesimal change of the mass density, is probed, however the change in density is produced.

For small wave vectors $\vec{q}$ the concept of mode Grüneisen parameters is not restricted to crystal lattices, but can also be applied to disordered condensed matter. As discussed in Section B.2, this holds true as long as the dimensions of spatial inhomogeneities of the material are small compared to the selected acoustic wavelength. Brillouin spectroscopy is especially well suited to determine mode Grüneisen parameters because it fulfils the required conditions. This technique measures the hypersonic frequencies f of a selected acoustic mode with a given polarization p at a constant wave vector $\vec{q}$, in linear response.

As stated in Section C.1, for soft matter with isotropic symmetry, the linear elastic behaviour is fully described by the longitudinally polarized acoustic mode and the degenerated transversely polarized acoustic mode. Only the longitudinal acoustic mode needs to be considered for isotropic liquids, as the shear modulus is zero. The desired changes of mass density introduced in eqn (9) are usually realized by variations of temperature or pressure.

For the present investigation, the temperature is the parameter that provokes simultaneously a variation of the frequency f_L of the longitudinally polarized acoustic mode and the mass density. In that case, the mode Grüneisen parameter of the longitudinally polarized hypersonic wave can be written as:

$$\gamma_L(T) = \delta_L(T)/\alpha(T), \quad (10)$$

where the volume thermal expansion coefficient is given by $\alpha(T) = -1/\rho\partial\rho/\partial T$, and $\delta_L(T) = -1/f_L\partial f_L/\partial T$ denotes the relative derivative with respect to the temperature of the hypersonic frequency f_L of the longitudinally polarized sound wave.

For the considered PNIPAM solutions with macroscopically isotropic symmetry, the mode Grüneisen parameter can be related to a combination c^+_{111} of the two independent TOECs c_{111} and c_{112} of isotropic liquids, according to:[21]

$$c^+_{111}(T) = c_{111}(T) + 2c_{112}(T) = -6c_{11}(T)(\gamma_L(T) + 5/6). \quad (11)$$

D Results and discussion

The longitudinal hypersonic frequencies *versus* temperature $f_L(T)$, determined by Brillouin spectroscopy, are indicated

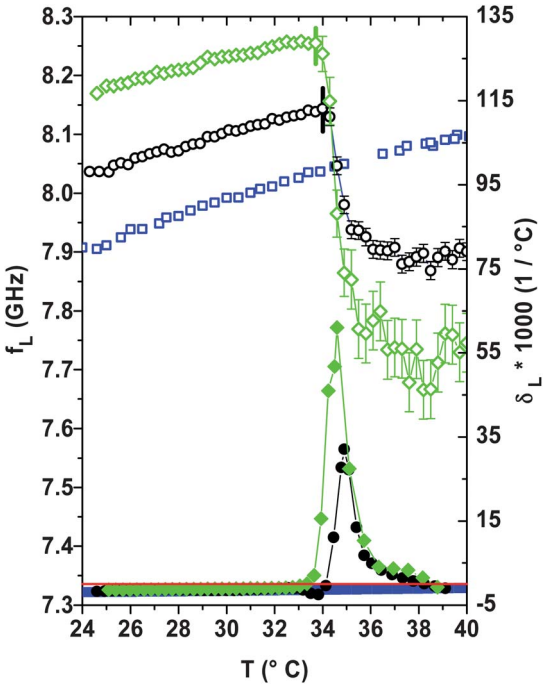

Fig. 1 Temperature evolution of the longitudinal hypersonic frequency $f_L(T)$ determined at the constant acoustic wave vector $q = 0.032$ nm^{-1} (open symbols) and of the relative temperature coefficient $\delta_L(T)$ (filled symbols) across the demixing transition. Squares: pure water, circles: 3 mass% PNIPAM solution and diamonds: 6 mass% PNIPAM solution. Vertical bars: T_c of the PNIPAM solutions. Horizontal line: $\delta_L(T) = 0$. Statistical error bars of $f_L(T)$ are smaller than the data points for transparent materials. They are enlarged above T_c for the opaque, demixed PNIPAM solutions due to highly increased elastic scattering. The $f_L(T)$-data are smoothed using cubic splines prior to calculation of the $\delta_L(T)$-curves.

across the demixing transition for two aqueous PNIPAM solutions and pure water in Fig. 1 (see open symbols). These datasets were obtained from the Brillouin spectra published in ref. 20. In the low-temperature phase, the absolute values of the hypersonic frequency $f_L(T)$, and hence the longitudinal modulus $c_{11}(T)$ (see eqn (5)), significantly rise with the PNIPAM concentration. At T_c, a steep, but continuous decrease of the hypersonic frequency $f_L(T)$ occurs for both PNIPAM solutions. It results from the mechanical instability related to the phase separation of the polymeric solutions into PNIPAM-rich and PNIPAM-poor domains.[20] This aspect will be discussed in more detail in the context of Fig. 4. Despite the on-going phase separation and the resulting opacity of the 3 and 6 mass% PNIPAM solutions above the demixing temperature, only one longitudinally polarized hypersonic wave is observed in this state. Consequently, the heterogeneous high-temperature phase behaves elastically homogeneous and isotropic on the length scale of the probed acoustic wavelength of about 200 nm. For these semi-dilute solutions, the PNIPAM-rich aggregates are thus much smaller than 200 nm. The hypersonic attenuation remains rather moderate and without significant variation around the demixing transition of all solutions.[20]

The relative temperature derivatives of the longitudinal hypersonic frequencies $\delta_L(T)$ are also depicted in Fig. 1 (see filled symbols) across the demixing transition for the PNIPAM

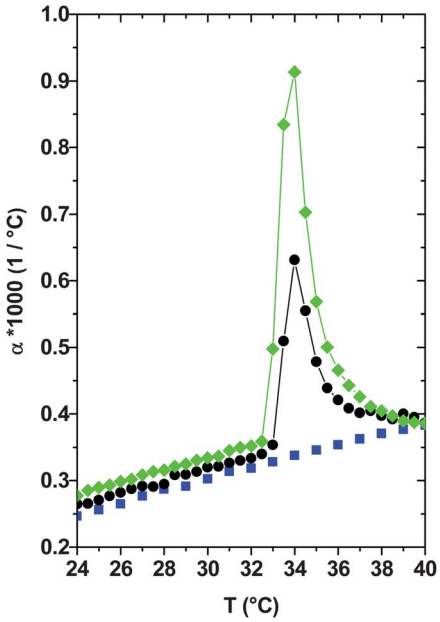

Fig. 2 Temperature evolution of the thermal expansion coefficient $\alpha(T)$ across the demixing transition, derived from density data.[20] Squares: pure water, circles: 3 mass% PNIPAM solution and diamonds: 6 mass% PNIPAM solution. Statistical error bars are smaller than data points.

solutions and pure water. The negative values of $\delta_L(T)$ for pure water result from the anomalous positive temperature dependence of $f_L(T)$, or $c_{11}(T)$, of water. This is attributed to the polyamorphism of this liquid.[60] Due to the dominant role of water within the low-temperature phase of the aqueous PNIPAM solutions, their $\delta_L(T)$-values are also negative. Above the demixing temperature T_c, pronounced positive $\delta_L(T)$-peaks arise in the phase-separating polymeric solutions. These peaks yield a hint for the occurrence of strong elastic nonlinearities related to the phase transition. The $\delta_L(T)$-values approach again that of water at about T_c + 5 °C.

The thermal expansion coefficients $\alpha(T)$ of the two PNIPAM solutions and pure water are depicted in Fig. 2 across the demixing transition. As expected, the volume expansion coefficient of water increases with temperature within the considered temperature interval. In the low-temperature phase the absolute values as well as the temperature dependence of $\alpha(T)$ of the aqueous PNIPAM solutions are very similar to those of water. However, the thermal expansion coefficients of both PNIPAM solutions show a pronounced peak, which spreads over a temperature interval of about 5 °C width above T_c. For temperatures above T_c + 5 °C, the thermal expansion coefficients of the PNIPAM solutions again approach those of water. Here, $\alpha(T)$ of the demixed solutions is dominated by that of the PNIPAM-poor phase, which possesses a thermal expansion coefficient being close to that of water. The pronounced $\alpha(T)$-peaks are related to the structural reorganization that occurs within the phase-separating solutions. Below the demixing temperature the PNIPAM chains are solvated by hydration shells.[35–37,46] Above T_c, these shells are repelled in a highly cooperative manner.[37,46] The amide groups of the PNIPAM side-chains form intra- and intermolecular hydrogen bonds with neighbouring amide groups in the course of the subsequent molecular aggregation. Infrared spectroscopy confirms that this phase separation occurs at least within a temperature interval of 4 to 5 °C width above T_c.[36]

According to the evolution of $\alpha(T)$, this structural reorganization obviously has a considerable impact on the average molecular interaction potentials. Hence, just above T_c, the thermal expansion coefficients are in fact dominated by

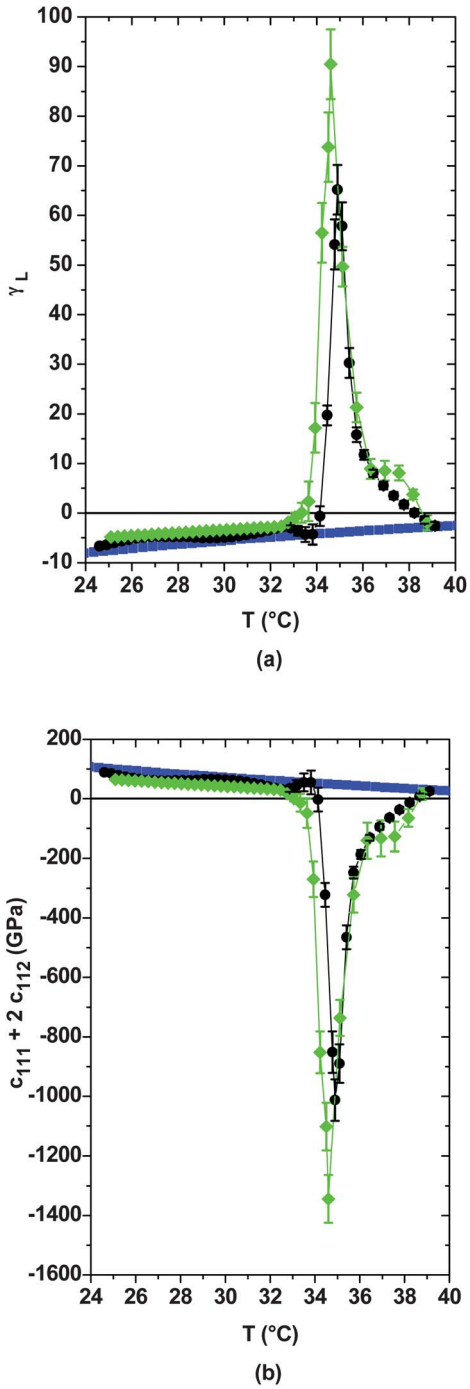

Fig. 3 Temperature evolution of (a) the longitudinal mode Grüneisen parameter $\gamma_L(T)$ and (b) the third order elastic constant $c^{+}_{111}(T) = c_{111}(T) + 2c_{112}(T)$ across the demixing transition. Squares: pure water, circles: 3 mass% PNIPAM solution, and diamonds: 6 mass% PNIPAM solution.

structural effects provoked by the demixing transition, rather than by purely thermal effects.

The values of mode Grüneisen parameters are usually positive for liquids and solids, and typically vary between 0 and 10.[16,17,21,26,27,53,54] Exceptions, which possess negative mode Grüneisen parameters, are oxide glasses[54] and water. The corresponding value of water, depicted in Fig. 3(a), is indeed negative and lies in between −10 and 0 for temperatures between 24 and 40 °C. These negative $\gamma_L(T)$-values result from the anomalous positive temperature dependence of $c_{11}(T)$ for water. As mentioned above, it is attributed to the polyamorphism of this liquid.[60] Due to the dominant role of water within the low-temperature phase of the aqueous PNIPAM solutions, their mode Grüneisen parameters are also negative and also vary between −10 and 0 (see Fig. 3(a)). Between T_c and T_c + 5 °C, the temperature dependence of $\gamma_L(T)$ drastically changes: pronounced positive peaks with maximal values of 60 or 90 arise. This underlines the important role of elastic nonlinearities during the transient structural reorganization occurring above T_c within the demixing polymeric solutions.

Using eqn (11), the TOECs c^+_{111} are evaluated in the same temperature zone for the three liquids. As depicted in Fig. 3(b), for water, positive values of c^+_{111} are observed. This is typical for a strain-hardening material like water. The strain-hardening effect decreases for the PNIPAM solutions on approaching T_c by heating, where it vanishes within the margin of error. This suggests that at the mechanical instability the strain-hardening due to water is compensated by the strain-softening related to the transition. The values of c^+_{111} get as small as −1000 ± 100 GPa and −1400 ± 100 GPa, respectively, at T_c + 1 °C for the 3 and 6 mass% PNIPAM solutions. Hence, an immense strain-softening emerges within a small temperature interval during the demixing of the PNIPAM solutions. Indeed, the TOECs determined for other elastically nonlinear materials, like ferroelastic crystals close to their ferroelastic phase transition or polymer melts, typically lie between −10 and −140 GPa.[15,18,23,24] Consequently, in the phase-separating PNIPAM solutions, $c^+_{111}(T)$ drastically exceeds the value of TOECs commonly measured. The strength and the sharpness of the c^+_{111}-peak reveals the important cooperativity of this phase transition.[37,46] Remarkably, c^+_{111} approaches again the typical values for water above T_c + 5 °C, which indicates that the tremendous elastic nonlinearity of −1400 GPa has faded away. This behaviour suggests that the TOECs more closely follow the evolution of the order parameter of the demixing transition than the SOECs. The elastic nonlinearities arise from the structural reorganisation, which is mainly governed by the modifications in H-bond interactions.[35,36] The large strain-softening actually endorses the formation of the demixed high-temperature state. In average the H-bonds continuously soften just above T_c.

Fig. 4 provides a comparison between the TOEC $c^+_{111}(T)$ and the SOEC $c_{11}(T)$ for the 6 mass% solution. The related values for water are indicated as a reference. The longitudinal moduli c_{11} are calculated according to eqn (5). As already mentioned, the isothermal compressibility $c^{-1}_{11}(T)$ is considered as one of the order parameter susceptibilities of the demixing transition of PNIPAM systems.[20,28,29] Accordingly, this demixing transition is

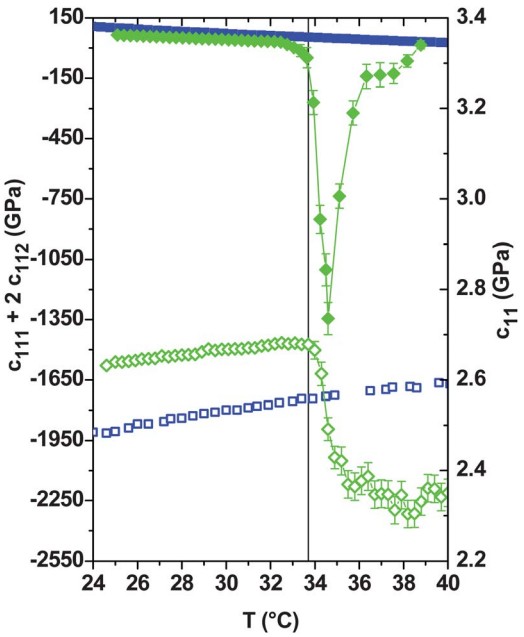

Fig. 4 Comparison between the temperature evolution of (a) the third order elastic constant $c^+_{111}(T) = c_{111}(T) + 2c_{112}(T)$ (filled symbols) and (b) the longitudinal modulus $c_{11}(T)$ (open symbols) across the demixing transition. Diamonds: 6 mass% PNIPAM solution and squares: pure water. Vertical line: T_c of the PNIPAM solution.

a ferroelastic-like transition for which the phase-separated high-temperature state is the ordered phase. In this phase the order parameter is non-zero and saturates with increasing temperature.[28] In line with this argumentation, the inverse order parameter susceptibility $c_{11}(T)$ shows a strong decrease upon heating the aqueous PNIPAM solution above T_c. Besides the elastic deformation, also the difference in polymer concentration in the demixing solution needs to be considered as an order parameter. The fluctuations of the polymer concentration interact with the deformation (or density) fluctuations and hence with the mechanical instability. However, no obvious change of the compressibility due to the critical concentration fluctuations[30] existing below the demixing transition could be resolved.[20,28,29] We hence surmise that the observed immense nonlinear elasticity in the demixing solutions is not dominated by concentration fluctuations.

The positive slopes of $c_{11}(T)$ for the PNIPAM solutions are similar to those of pure water. They are due to the polyamorphism of water. The significant softening of $c_{11}(T)$ for $T > T_c$ to values well below that of water is related to the strong modifications of the PNIPAM–water interactions at this mechanical instability.[20] The TOEC $c^+_{111}(T)$ obviously behaves totally different from the inverse order parameter susceptibility, $c_{11}(T)$, at the demixing transition. The alternative perspective gained by $c^+_{111}(T)$ provides quantitative insight into the strain-softening and the consecutive strain-hardening behaviour existing within the phase-separating solutions. The strain-softening endorses the destruction of the low-temperature phase and thus the formation of the phase-separated demixed state. The underlying reason for this strain-softening seems to reside

in strain fields, provoked by the smallest temperature variations, which interfere with variations of the molecular interactions in the vicinity of the demixing transition. In the phase-separating aqueous PNIPAM solutions, strain fields provoked by temperature variation seem to reinforce the cooperative release of the hydration shells of the PNIPAM molecules within a small temperature interval above the demixing temperature. The similarity between the cooperative hydration or dehydration of PNIPAM and peptide backbones in the aqueous environment[61] indicates that the role of nonlinear elasticity should not be underestimated for various biological systems. These findings substantiate that the common approach to focus mainly on linear elasticity at phase transitions within soft matter demands for reconsideration.

E Conclusions

The evolution of a third order (nonlinear) elastic constant is studied across the mechanical instability that accompanies the liquid–liquid demixing transition of aqueous PNIPAM solutions. Better understanding of this transition is achieved by the comparison of nonlinear with linear elastic constants at the transition. Therefore, the thermal evolution of the frequency of hypersonic waves and the mass density of semi-dilute aqueous PNIPAM solutions is investigated. Using the concept of mode Grüneisen parameters, for the first time the behaviour of a third order elastic constant across a liquid–liquid demixing transition is calculated. It turns out that the third order elastic constant of a 6 mass% PNIPAM solution changes from slightly positive values of about 50 GPa to immensely low, negative values of about −1400 GPa in the course of the phase separation before returning back to slightly positive values, when the order parameter of the demixing transition saturates. These negative values are an order of magnitude lower than those measured for other strain-softening materials at phase transitions. The changeover from a strain-hardening to a strongly strain-softening material reflects the evolution of the order parameter and accentuates the role of the mechanical instability present at this demixing transition.

Interestingly, the third order elastic constants, rather than the second order elastic constants, strongly endorse the formation of the demixed high-temperature state. It seems that strain fields, provoked by the smallest temperature variations, which interfere with variations of the molecular interactions within the phase-separating solutions, are the reason for the strain-softening. The investigation evidences the need for addressing fundamental questions related to the universal role played by elastic nonlinearities at phase transitions within soft materials.

Acknowledgements

We thank O. Astasheva for technical support and C.M. Papadakis for fruitful discussions. M.P. thanks the Fonds National de la Recherche (Luxembourg) for receipt of a Marie Curie co-funded AFR Postdoc grant (FP7-Cofund AFR-PDR 2010-2, 1036107). P.M.B. acknowledges financial support by the Deutsche Forschungsgemeinschaft DFG, priority program SPP1259 'Intelligente Hydrogele' (grant MU1487/8).

Notes and references

1 C. P. Broedersz, C. Storm and F. C. MacKintosh, *Phys. Rev. Lett.*, 2008, **101**, 118103.
2 C. Storm, J. J. Pastore, F. C. MacKintosh, T. C. Lubensky and P. A. Janmey, *Nature*, 2005, **435**, 191–194.
3 T. Tanaka, S. T. Sun, Y. Hirokawa, S. Katayama, J. Kucera, Y. Hirose and T. Amiya, *Nature*, 1987, **325**, 796–798.
4 C. P. Broedersz, K. E. Kasza, L. M. Jawerth, S. Muenster, D. A. Weitz and F. C. MacKintosh, *Soft Matter*, 2010, **6**, 4120–4127.
5 Y.-C. Lin, G. H. Koenderink, F. C. MacKintosh and D. A. Weitz, *Soft Matter*, 2011, **7**, 902–906.
6 G. Romeo, A. Fernandez-Nieves, H. M. Wyss, D. Acierno and D. A. Weitz, *Adv. Mater.*, 2010, **22**, 3441.
7 L. Golubovic and T. C. Lubensky, *Phys. Rev. Lett.*, 1989, **63**, 1082–1085.
8 Y. Park, C. A. Best, T. Kuriabova, M. L. Henle, M. S. Feld, A. J. Levine and G. Popescu, *Phys. Rev. E: Stat., Nonlinear, Soft Matter Phys.*, 2011, **83**, 051925.
9 H. Wada, Y. Murayama and M. Sano, *Phys. Rev. E: Stat., Nonlinear, Soft Matter Phys.*, 2005, **72**, 041803.
10 A. V. Dobrynin and J.-M. Y. Carrillo, *Macromolecules*, 2011, **44**, 140–146.
11 Y. Z. Wang, B. H. Li, X. M. Xiong, B. Wang and J. X. Zhang, *Soft Matter*, 2010, **6**, 3318–3324.
12 B. Yohsuke, K. Urayama, T. Takigawa and K. Ito, *Soft Matter*, 2011, **7**, 2632–2638.
13 M. Guvendiren, H. D. Lu and J. A. Burdick, *Soft Matter*, 2012, **8**, 260–272.
14 Q. Wen, A. Basu, P. A. Janmey and A. G. Yodh, *Soft Matter*, 2012, **8**, 8039–8049.
15 J. K. Krüger, C. Grammes, K. Stockem, R. Zietz and M. Dettenmaier, *Colloid Polym. Sci.*, 1991, **269**, 764–771.
16 U. Müller, M. Philipp, R. Bactavatchalou, R. Sanctuary, J. Baller, B. Zielinski, W. Possart, P. Alnot and J. K. Krüger, *J. Phys.: Condens. Matter*, 2008, **20**, 205101.
17 J. K. Krüger, K. P. Bohn and J. Schreiber, *Phys. Rev. B: Condens. Matter Mater. Phys.*, 1996, **54**, 15767–15772.
18 K. Kadowaki and M. Matsukawa, *2005 IEEE Ultrasonics Symposium*, 2005, vol. 1–4, pp. 2116–2119.
19 D. Cavaille, C. Levelut, R. Vialla, R. Vacher and E. Le Bourhis, *J. Non-Cryst. Solids*, 1999, **260**, 235–241.
20 M. Philipp, U. Müller, R. Aleksandrova, R. Sanctuary, P. Müller-Buschbaum and J. K. Krüger, *Soft Matter*, 2012, **8**, 11387.
21 G. Grimvall, *Thermophysical Properties of Materials*, North-Holland Physics Publishing, Amsterdam, 1986.
22 E. K. H. Salje, *Phase transitions in ferroelastic and co-elastic crystals. An introduction for mineralogists, material scientists and physicists*, Cambridge University Press, Cambridge, 1990.
23 E. L. Meeks and R. T. Arnold, *Phys. Rev. B: Solid State*, 1970, **1**, 982.
24 W. W. Cao, G. R. Barsch, W. H. Jiang and M. A. Breazeale, *Phys. Rev. B: Condens. Matter Mater. Phys.*, 1988, **38**, 10244–10255.

25 J. Shanker and W. N. Bhende, *Phys. Status Solidi B*, 1986, **136**, 11–30.
26 E. M. Brody, C. J. Lubell and C. L. Beatty, *J. Polym. Sci., Polym. Phys. Ed.*, 1975, **13**, 295–301.
27 J. K. Krüger, K. P. Bohn, M. Pietralla and J. Schreiber, *J. Phys.: Condens. Matter*, 1996, **8**, 10863–10874.
28 S. Hirotsu, *Phase Transitions*, 1994, **47**, 183–240.
29 S. Hirotsu, I. Yamamoto, A. Matsuo, T. Okajima, H. Furukawa and T. Yamamoto, *J. Phys. Soc. Jpn.*, 1995, **64**, 2898–2907.
30 A. Meier-Koll, V. Pipich, P. Busch, C. M. Papadakis and P. Müller-Buschbaum, *Langmuir*, 2012, **28**, 8791–8798.
31 M. Shibayama, T. Tanaka and C. C. Han, *J. Chem. Phys.*, 1992, **97**, 6829–6841.
32 C. Scherzinger, O. Holderer, D. Richter and W. Richtering, *Phys. Chem. Chem. Phys.*, 2012, **14**, 2762–2768.
33 J. Adelsberger, A. Kulkarni, A. Jain, W. Wang, A. M. Bivigou-Koumba, P. Busch, V. Pipich, O. Holderer, T. Hellweg, A. Laschewsky, P. Müller-Buschbaum and C. M. Papadakis, *Macromolecules*, 2010, **43**, 2490–2501.
34 J. Adelsberger, E. Metwalli, A. Diethert, I. Grillo, A. M. Bivigou-Koumba, A. Laschewsky, P. Müller-Buschbaum and C. M. Papadakis, *Macromol. Rapid Commun.*, 2012, **33**, 254–259.
35 B. Sun, Y. Lin, P. Wu and H. W. Siesler, *Macromolecules*, 2008, **41**, 1512–1520.
36 Y. Maeda, T. Higuchi and I. Ikeda, *Langmuir*, 2000, **16**, 7503–7509.
37 F. Tanaka, T. Koga and F. M. Winnik, *Prog. Colloid Polym. Sci.*, 2009, **136**, 1–8.
38 S. Koizumi, M. Monkenbusch, D. Richter, D. Schwahn and B. Farago, *J. Chem. Phys.*, 2004, **121**, 12721–12731.
39 W. Wang, K. Troll, G. Kaune, E. Metwalli, M. Ruderer, K. Skrabania, A. Laschewsky, S. V. Roth, C. M. Papadakis and P. Müller-Buschbaum, *Macromolecules*, 2008, **41**, 3209–3218.
40 W. Wang, G. Kaune, J. Perlich, C. M. Paradakis, A. M. B. Koumba, A. Laschewsky, K. Schlage, R. Roehlsberger, S. V. Roth, R. Cubitt and P. Müller-Buschbaum, *Macromolecules*, 2010, **43**, 2444–2452.
41 J. K. Cho, Z. Meng, L. A. Lyon and V. Breedveld, *Soft Matter*, 2009, **5**, 3599–3602.
42 V. Tokarova, A. Pittermannova, J. Cech, P. Ulbrich and F. Stepanek, *Soft Matter*, 2012, **8**, 1087–1095.
43 Y. Liu, Z. Li and D. Liang, *Soft Matter*, 2012, **8**, 4517–4523.
44 P. Kujawa and F. M. Winnik, *Macromolecules*, 2001, **34**, 4130–4135.
45 Y. Satokawa, T. Shikata, F. Tanaka, X.-p. Qiu and F. M. Winnik, *Macromolecules*, 2009, **42**, 1400–1403.
46 H. Kojima and F. Tanaka, *Macromolecules*, 2010, **43**, 5103–5113.
47 M. A. Molina, C. R. Rivarola, M. F. Broglia, D. F. Acevedo and C. A. Barbero, *Soft Matter*, 2012, **8**, 307–310.
48 C. Fernandez-Lopez, C. Perez-Balado, J. Perez-Juste, I. Pastoriza-Santos, A. R. de Lera and L. M. Liz-Marzan, *Soft Matter*, 2012, **8**, 4165–4170.
49 S. Sun and P. Wu, *Soft Matter*, 2011, **7**, 7526–7531.
50 T. Hellweg, C. D. Dewhurst, W. Eimer and K. Kratz, *Langmuir*, 2004, **20**, 4330–4335.
51 M. Karg, I. Pastoriza-Santos, J. Perez-Juste, T. Hellweg and L. M. Liz-Marzan, *Small*, 2007, **3**, 1222–1229.
52 N. Greinert and W. Richtering, *Colloid Polym. Sci.*, 2004, **282**, 1146–1149.
53 K. Brugger and T. C. Fritz, *Phys. Rev.*, 1967, **157**, 524.
54 R. J. Wang, W. H. Wang, F. Y. Li, L. M. Wang, Y. Zhang, P. Wen and J. F. Wang, *J. Phys.: Condens. Matter*, 2003, **15**, 603–608.
55 J. R. Sandercock, in *Light Scattering in Solids III. Recent Results*, ed. M. Cardona and G. Guntherodt, Springer, Berlin, 1982.
56 M. Philipp, U. Müller, R. Sanctuary, P. Seck and J. Krüger, *Scanning Brillouin Microscopy: Acoustic Microscopy at Gigahertz Frequencies*, Institut Grand-Ducal de Luxembourg, Luxembourg, 2011.
57 M. Philipp, F. Collette, M. Veith, P. Seck, R. Sanctuary, U. Müller, J. Kieffer and J. K. Krüger, *J. Phys. Chem. B*, 2009, **113**, 12655–12662.
58 M. Philipp, U. Müller, R. Sanctuary, J. Kieffer, W. Possart and J. K. Krüger, *Soft Matter*, 2011, **7**, 118–124.
59 C. Kittel, *Introduction to solid state physics*, 4th edn, 1971.
60 M. C. Bellissent-Funel and L. Bosio, *J. Chem. Phys.*, 1995, **102**, 3727–3735.
61 A. Oleinikova and I. Brovchenko, *J. Phys. Chem. Lett.*, 2011, **2**, 765–769.